analytical chemistry

pubs.acs.org/ac
Article

Fast NMR-Based Assessment of Cancer-Associated Protein Glycosylations from Serum Samples

Lorena Rudolph, Renia Krellmann, Darko Castven, Lina Jegodzinski, Helena Deriš, Jerko Štambuk, Jarne Mölbitz, Luna Dechent, Kai Sperling, Melissa Lindloge, Nele Friedrich, Franziska Schmelter, Bandik Föh, Irena Trbojević-Akmačić, Christian Sina, Matthias Nauck, Astrid Petersmann, Jens U. Marquardt, Ulrich L. Günther,* and Alvaro Mallagaray*

Cite This: *Anal. Chem.* 2025, 97, 9367−9377

Read Online

ACCESS | Metrics & More | Article Recommendations | Supporting Information

ABSTRACT: Nuclear magnetic resonance (NMR) spectra of blood serum and plasma show signals arising from metabolites, lipoproteins, and *N*-acetyl methyl groups of *N*-glycans covalently linked to acute-phase proteins. These glycan signals often called glycoprotein A (GlycA) and glycoprotein B (GlycB) arise from *N*-acetyl methyl groups and have been proposed as biomarkers, initially for cardiovascular diseases, but also for other inflammatory conditions. For the detection of glycan resonances, *J*-edited, diffusion, and relaxation filtered NMR spectroscopy (JEDI) has been proposed to suppress the lipoprotein signals. JEDI is however limited to measure those acetyl signals, whereas all other glycan resonance cannot be observed. For improved glycoprotein profiling, the signals arising from the pyranose ring protons are essential. Here, we show how selective frequency excitation combined with scalar coupling filtering can be used to dramatically increase the number of *N*-glycan signals observable in NMR spectra of serum and plasma samples, facilitating glycosylation profiling in less than 30 min. This approach grants selective detection of sialylation, galactosylation, *N*-acetylglucosaminylation, and fucosylation of dominant *N*-glycans and, to some extent, *N*-glycan branching complexity. Notably, sialylated and nonsialylated Lewis^x and Lewis^a antigens can also be observed. Lewis^a antigen is well established as a cancer biomarker, known as CA19-9. NMR glycosylation profiles from nine isolated serum glycoproteins show excellent agreement with well-established UHPLC-MS analysis. The proposed NMR method facilitates the detection of glycoprotein biomarkers without the need for enzymatic treatment of serum or plasma and provides a robust read-out as exemplified by samples from 33 patients with hepatocellular carcinoma.

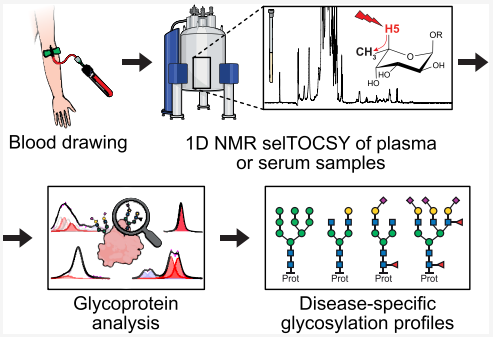

INTRODUCTION

Protein glycosylation is the most common posttranslational modification in human cells, resulting in a diverse array of glycoconjugates. Glycan synthesis is a dynamic process highly influenced by the surrounding environment, including enzyme activity, carbohydrate precursors, organelle structures, specific cell types, and cellular signaling pathways. Glycans are involved in a myriad of functions both in physiological and pathological states.[1−3] Aberrant glycosylations in circulating proteins have been observed in many inflammation-related diseases, including cardiovascular disease,[4] Parkinson's disease,[5−7] Alzheimer's disease,[8,9] inflammatory bowel disease (IBD),[10,11] metabolic dysfunction-associated steatotic liver disease (MASLD), and its progression into hepatocellular carcinoma (HCC).[12]

Acute-phase inflammation proteins are characterized by their robust response to inflammation, mediated by interleukin (IL)-1, -6, and -8, resulting in significant increases or decreases in their blood concentrations (at least 25%). Moreover, the vast majority of acute-phase proteins have one or more glycosylation sites. Several acute-phase proteins and their associated glycosylation profiles are used as potent diagnostic parameters for cancer[13] due to neoplasia-induced hepatic reprogramming.[14−16] For instance, the well-established serological biomarker CA19-9—also known as sialyl Lewis^a or sLe^a—is known to increase in various cancers, including gastrointestinal and pancreatic cancer.[17,18] A similar glycan antigen, sialyl Lewis^x (sLe^x), has also been shown to represent a valuable marker in cancers[19] for prognosis and treatment response.[20]

However, the clinical utility of these markers is significantly hampered by the analytical complexity involved in assessing

Received: January 13, 2025
Revised: March 21, 2025
Accepted: March 28, 2025
Published: April 25, 2025

https://doi.org/10.1021/acs.analchem.5c00285
Anal. Chem. 2025, 97, 9367−9377

protein glycosylation. Clinical analysis relies on immunoassays, employing antibodies directed against specific glycosylation markers such as sLe[a], which tend to show variation in binding specificity with consequences for clinical interpretation.[21,22] While mass spectrometric (MS) analyses offer the most comprehensive option to identify glycosylation biomarkers,[3,23] the cost of MS glycoproteomics is too high for routine clinical use.[24]

Nuclear magnetic resonance (NMR) spectroscopy has often been used to decipher glycan structures in native proteins, usually employing two-dimensional (2D) spectra in combination with chaotropic agents[25] and/or isotope incorporation.[26] Screening of biologic fluids is usually implemented using simple and fast one-dimensional (1D) spectra. From NMR analysis of blood serum or plasma, one can now obtain ca. 40 metabolite concentrations and a range of lipoprotein subclass parameters with triglyceride and cholesterol content.[27,28] Currently, the concentration of blood glycoprotein *N*-glycan is assessed employing two prominent signals seen in 1D-NOESY spectra at around 2.0 ppm originating from *N*-acetyl methyl groups. These signals are commonly referred to as glycoprotein A (GlycA)[29] and glycoprotein B (GlycB)[30] and originate from *N*-acetyl methyl groups of neuraminic acid (Neu5Ac) and *N*-acetylglucosamine (GlcNAc), respectively.[31] Multiple studies have provided compelling evidence that alterations in GlycA/B profiles correlate with a variety of medical conditions,[32−36] supporting the paradigm that GlycA/B NMR signatures can serve as clinically valuable biomarkers for inflammation-related diseases.

Here, we show how selective frequency excitation combined with signal filtering based on scalar coupling can be used to obtain glycosylation profiles of the most abundant acute-phase proteins in blood in less than 30 min. No additional sample preparation is required, and buffers are compatible with those commonly used for metabolite and lipoprotein quantification.[37] This methodology allows the identification of altered *N*-glycosylation patterns, including linkage-specific sialylation levels, galactosylation, *N*-acetylglucosaminylation, fucosylation (including Lewis[x] and Lewis[a] antigens), and branching complexity of most abundant *N*-glycans. This approach also allows the selective observation of the ethyl groups from phosphatidylcholines (PC)—previously identified via their $N(CH_3)_3$ methyl groups—often termed supramolecular phospholipids composite signal (SPC).[36] SPC has been correlated with cardiovascular risk in COVID-19 patients.[38]

In this article, the scope of the method is illustrated using a collection of nine acute-phase proteins isolated from human serum. NMR glycosylation profiles are compared to glycosylation profiles obtained by UHPLC-MS, showing excellent correlations for the most abundant glycans. As will be shown, spectral overlap with metabolite and lipoprotein signals could be largely eliminated by fine-tuning acquisition parameters. The clinical relevance is demonstrated using samples from a cohort of 33 HCC patients and 20 healthy controls. NMR spectra of serum samples reveal distinct glycosylation profiles in HCC patients, with increased concentrations of Lewis[x] (Le[x]) and/or Lewis[a] (Le[a]) antigen along with altered α2,3- to α2,6-sialylation ratios. The PC marker was also found to be downregulated in HCC patient samples. Multivariate and univariate analyses demonstrate the quality of the NMR glycoprotein profile (HCC vs controls, AUROC 100%). While this NMR approach will never be as comprehensive as MS analysis, it provides a fast, robust, and information-rich glycosylation signature free of the limitations associated with antibody-based tests.

MATERIALS AND METHODS

Detailed protocols for every experiment are included in the Supporting Information accompanying this manuscript.

Glycans. *N*-glycans, histo-blood group antigens (HBGA), and Lewis antigens were commercially acquired or kindly donated by collaborators. For more details, see Table S1. Glycans were dissolved in D_2O and lyophilized prior to NMR sample preparation.

Isolation of Acute-Phase Proteins from Human Serum. Serum glycoproteins were isolated by flotation ultracentrifugation (UC) by adjusting the density to 1.3860 g/mL with NaBr followed by ultracentrifugation at 40.000 rpm for at least 72 h at 20 °C.[31,39] Pellet was dialyzed against a solution containing 50 mM sodium phosphate, pH 7.30, and 100 mM NaCl at 6 °C. For the isolation of individual acute-phase proteins, serum glycoproteins were thawed at room temperature for 30 min. Buffer was exchanged to 20 mM Tris-HCl or sodium phosphate buffer, pH 7.0−8.0 containing 0−150 mM NaCl, and the solution and injected onto the column equilibrated in the same buffer. Desired acute-phase proteins were eluted according to column vendor protocols (see the Supporting Information for more details).

Quantification of Acute-Phase Proteins from Serum Samples. HSA, HP, complement factors C3 and C4, TF, CP, AAT, C-reactive protein (CRP), α-fetoprotein (AFP), IgG, IgA, and immunoglobulins M (IgM) were measured in thawed serum samples by a polychromatic (600, 540, and 700 nm) end-point technique for albumin and nephelometric methods for the remaining proteins using the defined standard assays on a Dimension Vista 1500 Intelligent Lab System (Siemens Healthcare Diagnostics, Eschborn, Germany). ELISA commercial kits Clusterin (Biolab Assays, BA3001), α1-acid glycoprotein (AGP) (Quantine ELISA, DAGP00), and CFH (HycultBiotech, HK342) were used to quantify the corresponding proteins with a Tecan Infinite F50.

Glycoprofiling of Isolated Glycoproteins by UHPLC-MS. Glycoprofiling of isolated glycoproteins by UHPLC-MS was obtained following a previously described protocol[40] with the following variations: 25 μL of isolated glycoprotein samples in 20 mM sodium phosphate, 50 mM NaCl, pH 7.3 were dried in a vacuum centrifuge, resuspended in 30 μL of 13.3 g/L sodium dodecyl sulfate, and incubated at 65 °C for 10 min. Labeled glycans were cleaned on a hydrophilic 0.2 μm AcroPrep wwPTFE filter plate (Pall Corporation), and glycans were eluted from the plate with 2 × 90 μL of ultrapure water. *N*-Glycans from isolated glycoproteins were annotated following a modification of a reported protocol.[41] The differences are ionBooster source vaporizer temperature set to 300 °C and sheath gas flow set to 300 Nl/h, and mass spectra were recorded in the range 50−2750 m/z with a frequency of 0.5 Hz. The LC-MS system was under the control of HyStar 4.1 software, and spectra were analyzed in Bruker Data analysis 4.4.

Preparation of NMR Samples. NMR samples from reference glycans and isolated glycoproteins were prepared in 1.7 mm (40 μL) or in 3 mm (160 μL) NMR tubes. Enzyme reactions with isolated proteins were conducted in 3 mm NMR tubes. Buffer composition varied among samples as described in the Supporting Information, pg. S-5. Experiments with serum and plasma samples were conducted in 5 mm NMR

https://doi.org/10.1021/acs.analchem.5c00285
Anal. Chem. 2025, 97, 9367−9377

tubes (600 μL). These samples were prepared in accordance with Bruker SOPs. The composition of the IVDr NMR buffer corresponds to the buffer used by Bruker in its in vitro diagnostic platform.[37]

NMR Experiments. All experiments with reference glycans and isolated acute-phase proteins were acquired in a Bruker Avance III HD 600 MHz spectrometer equipped with TCI cryogenic probe or in a Bruker Avance III HD 600 MHz spectrometer equipped with a TCI Microcryoprobe. Human serum and plasma samples along with enzyme reactions were measured in a Bruker Avance III HD 600 MHz NMR spectrometer equipped with a TXI room temperature probe and Bruker SampleJet automatic sample exchanger with sample storage set at 6 °C. All experiments were acquired at 310 K. Spectra from reference glycans, isolated glycoproteins, and enzyme reactions were processed with TopSpin 4.0.7 (Bruker). NMR spectra from serum samples were processed with Topspin 3.6.3 except for selTOCSY experiments, which were processed and analyzed using an in-house Matlab 2022a script.

1D NMR experiments were acquired in full automation. All pulse sequences refer to Bruker standard library. For the measurement of metabolites, lipoproteins and GlycA/B concentrations the following experiments were acquired: ^{1}H-NOESY (*noesygppr1d*), ^{1}H-CPMG (*cpmgpr1d*), and JEDI-PGPE[42] (*zgpezf.ivdr*). Experiments were automatically processed according to Bruker SOPs, small molecules were quantified using the Bruker IVDr Quantification in Plasma/Serum Analysis (B.I.Quant-PS2.0), and lipoprotein fractions and subclasses thereof were quantified using the Bruker IVDr Lipoprotein Subclass Analysis (B.I.LISATM). Glycosylation markers were obtained from selTOCSY experiments (*selmlgp.2*). Experimental setup and spectral processing are described in the Supporting Information, pg. S-6. After Fourier transform, spectra were calibrated, zero-order phase corrected, baseline corrected, and Voigt lineshapes were fitted under selected areas to obtain glycosylation profiles and to quantify SPE-1 and SPE-2 signals. See the Supporting Information, pg. S-7 and Figure S35 for more details on lineshape fitting. The modified version of selTOCSY used to measure ^{1}H-T_1 relaxation times and data analysis are described in the Supporting Information, pg S-6.

2D NMR experiments acquired for the assignment of reference glycans and isolated glycoproteins were: ^{1}H,^{13}C-edited-HSQC (*hsqcedetgpsisp2.2*), ^{1}H,^{1}H-TOCSY (*mlevesgpph*), ^{1}H,^{1}H-ROESY (*roesyesgpph*), and/or ^{1}H,^{1}H-NOESY (*noesyesgpph*). For more details on the experimental setup, see Table S2.

Enzyme Digestions Followed by NMR. Glycoprotein samples were diluted to a maximum of 50 mg/mL glycoprotein concentration after enzyme addition. Serum samples were diluted 50% with IVDr NMR buffer.[37] A detailed list of the enzymes used in this study can be found in Table S3. Reactions were conducted at 37 °C and monitored by ^{1}H-CPMG and selTOCSY NMR experiments until no further reaction product was formed. A reference sample was incubated in the absence of enzymes under identical conditions. Released carbohydrates were removed by size exclusion using 7 kDa molecular weight cutoff Zeba Spin desalting columns (Thermo Scientific, ref 89890).

Statistical Analysis. To determine statistically significant differences between healthy controls and HCC patients, Mann–Whitney U tests using the false discovery method of Benjamini, Krieger, and Yekutiele (Q = 0.05) were performed for the area under the fitted curves (AUC), concentrations of acute-phase proteins, and relative concentrations of *N*-glycans. Fitted AUCs of the same spectral region with a q-value (corrected p-value) < 0.01 were summed up and used as new features. For principal component analysis (PCA), the data were preprocessed with Pareto scaling and mean centering. For orthogonal partial least-squares discriminant analysis (O-PLS-DA), the data were preprocessed with orthogonal signal correction, Pareto scaling, and mean centering. Venetian blinds were used as a cross-validation method with 10 data splits, one sample per blind, and 10% left-out data. A permutation test with 100 iterations was performed for the O-PLS-DA. Spearman correlation coefficients were calculated, and significance was tested using a two-tailed approach. PCA and O-PLS-DA were performed in the PLS_Toolbox software package, version 9.1, from Eigenvector Research running in a Matlab 2022a software package. All other statistical analyses were performed using in-house scripts running in a Matlab 2022a software package.

RESULTS AND DISCUSSION

Hidden Topology of Glycoprotein *N*-Glycan NMR Signals in Human Serum. Standard 1D-NOESY spectra of serum and plasma samples are dominated by metabolites, proteins, and lipoproteins, leaving *N*-acetyl methyl groups from Neu5Ac and GlcNAc moieties (GlycA and GlycB, respectively) as the only observable *N*-glycan signals (Figure 1A).

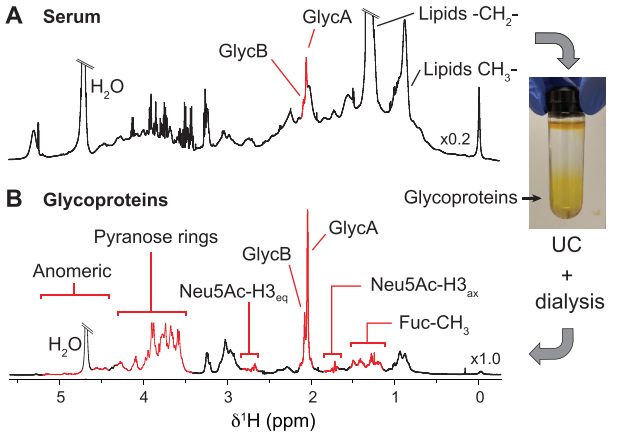

Figure 1. Identification of *N*-glycan signals in NMR spectra from human serum. (A) 1D-NOESY spectrum of serum. (B) Ultracentrifugation of serum followed by the removal of metabolites using dialysis allows isolation of serum glycoproteins. A CPMG spectrum of isolated glycoproteins allows the identification of *N*-glycan signals, here highlighted in red.

Initially, we used UC to prepare an acute-phase protein reference sample from blood serum devoid of any lipoproteins. Following UC, residual metabolites were removed by dialysis, yielding highly concentrated serum acute-phase glycoproteins suitable for NMR analysis. NMR spectra of this sample were dominated by a strong protein background, which were removed by Carr–Purcell–Meiboom–Gill (CPMG) sequences serving as T_2-filters.

The removal of lipoproteins and metabolites exposed a series of signals corresponding to *N*-glycans decorating acute-phase proteins (red in Figure 1B), demonstrating that NMR spectra of serum harbor a vast, yet largely unexplored array of *N*-glycan signals, beyond GlycA and GlycB, mainly arising

https://doi.org/10.1021/acs.analchem.5c00285
Anal. Chem. 2025, 97, 9367−9377

from pyranose ring protons and methyl groups. Assignment of these signals can unveil a new type of glycosylation marker with significant diagnostic potential. To selectively detect glycosylation in blood sera or plasma using NMR, the challenge lies in isolating glycan signals with minimal or no sample preparation. To address this, we have employed selective TOCSY experiments.

Selective TOCSY Experiments Reveal Serum and Plasma *N*-Glycan Signals. NMR offers a range of methods to filter out unwanted signals, including *J*-editing, diffusion, and relaxation filtering, which can be tuned to efficiently remove metabolite and protein signals. However, they also suppress the majority of *N*-glycan signals, thereby restricting their detection primarily to GlycA and GlycB.[36] Despite the advancements, these methods fail to eliminate lipid CH_2 signals, which overlap with critical *N*-glycan spectral features such as cancer-associated fucose methyl (Fuc-CH_3) signals from Lewis antigens (Figure 1).

Selective excitation combined with scalar coupling-based signal filtering, also known as selective TOCSY (selTOCSY), represents an excellent alternative to overcome these challenges (Figure S1). SelTOCSY is a robust and well-established NMR technique, amenable for automation in a high-throughput analytical setup. Additionally, TOCSY transfer efficiently removes the protein background, rendering T_2 filters unnecessary. This approach does not require any special sample handling, hence enabling the elucidation of unique glycosylation profiles directly from untreated serum and plasma samples.

SelTOCSY involves excitation of selected *N*-glycan proton resonances followed by through-bond magnetization transfer to the "reporter" protons, from which *N*-glycans can be profiled (Figure 2A). Selection of frequencies for selective excitation is based on a reference spectral library of the most abundant human serum *N*-glycans measured under the conditions typically used for quantification of serum metabolites and lipoproteins (Table S1 and experimental details in the Supporting Information).[37] Our current library includes 22 complex-type *N*-glycans, 6 high-mannose *N*-glycans, 6 human histo-blood group antigens (HBGAs), 4 nonsialylated, and 2 sialylated Lewis antigens (Le and sLe, respectively). Glycan signal assignments and coupling constants are detailed in Figures S2−S9 and Tables S4−S6. Signals showing characteristic chemical shifts for distinctive *N*-glycans—known as structural reporter groups[43]—were selected and used for glycan identification from complex mixtures.

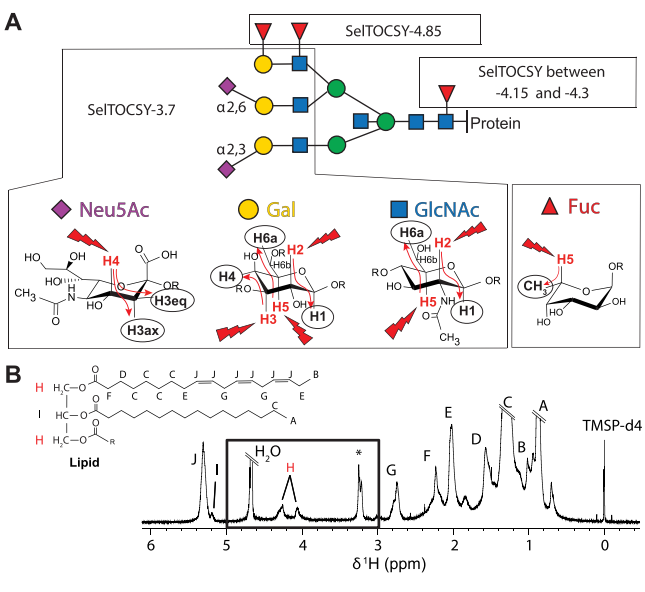

Figure 2. (A) Cartoon of a representative *N*-glycan and structures of the individual carbohydrates, with red bolt symbols indicate the hydrogens selectively excited and black circles indicate the observed protons in selTOCSY experiments. Red arrows indicate the magnetization transfer during the TOCSY mixing time. (B) Spectrum of human blood lipids isolated by UC. Signal assignments are indicated with capital letters. The black square indicates the ideal frequency range for selective *N*-glycan excitation. * denotes −N(Me_3) from PC.

The key to this strategy is the elimination of broad methyl (ca. 0.9 ppm) and ethyl (ca. 1.3 ppm) lipid signals superimposed to Fuc-CH_3 signals (Figure 2B, signals A to C). Selective excitation between 3 and 5 ppm followed by TOCSY transfer yields spectra entirely devoid of lipid signals, even after the addition of substantial amounts of lipids isolated from human serum (Figure S10). Lipid resonances in this frequency range are not observed because they correspond to glycerol hydrogens, from which magnetization is not transferred to the aliphatic chains in TOCSY sequences (Figure S11). This frequency range is ideal for the generation of glycan signals, as it encompasses a spectral region where signals from pyranose hydrogens are typically found.

Assignment of *N*-Glycan Signals from Serum and Plasma in selTOCSY Experiments. We have identified three frequencies within the range of 3−5 ppm that allow the observation of glycan structural reporter groups. Selective excitation at 3.7 ppm reveals equatorial and axial H3 signals of Neu5Ac, along with anomeric protons of galactoses (Gal) and GlcNAc located in the antennae (Figure 3A). The areas under the curve (AUC) of Neu5Ac-H3 signals align perfectly with GlycA, a marker classically used to evaluate total Neu5Ac content (Figure S12). Selective excitation between 4.15 and 4.3 ppm reveals methyl signals from fucoses (Fuc) situated in the *N*-glycan core (Figure 3B). Finally, selective excitation at 4.85 ppm uncovers methyl signals from Fuc being part of Lewis antigens (Figure 3C). To note, selTOCSY does not differentiate between sialylated and nonsialylated Lewis antigens. Therefore, (s)Le will be used to describe both forms of Lewis antigens. These three frequencies will be referred to as selTOCSY-3.7, -4.3, and -4.85 throughout this manuscript. Core GlcNAc cannot be observed for the vast majority of serum glycoproteins due to fast R_2 relaxation.[31,44] Further details on signals assignment can be found in the Supporting Information, pg. S-22.

SelTOCSY also allows the observation of potential biomarkers beyond protein *N*-glycosylation. Studies have shown that the total concentration of PC can be quantified from the supramolecular phospholipid composite (SPC-Me_3) arising from trimethylammonium methyl groups from choline.[36,38,42] SelTOCSY-3.7 yields a prominent signal at approximately 4.2 ppm, corresponding to the −O−CH_2− ethoxy group of PC (identified as supramolecular phospholipid ethylene signal or SPE-1 in orange in Figure 3A). Similarly, selTOCSY-4.3 generates a distinct signal at approximately 3.7 ppm, originating from the −N−CH_2− group from PC (indicated as SPE-2 in orange in Figure 3B). To note, SPE-1 and -2 from selTOCSY show excellent correlation with the SPC marker classically measured in JEDI experiments used to

https://doi.org/10.1021/acs.analchem.5c00285
Anal. Chem. 2025, 97, 9367−9377

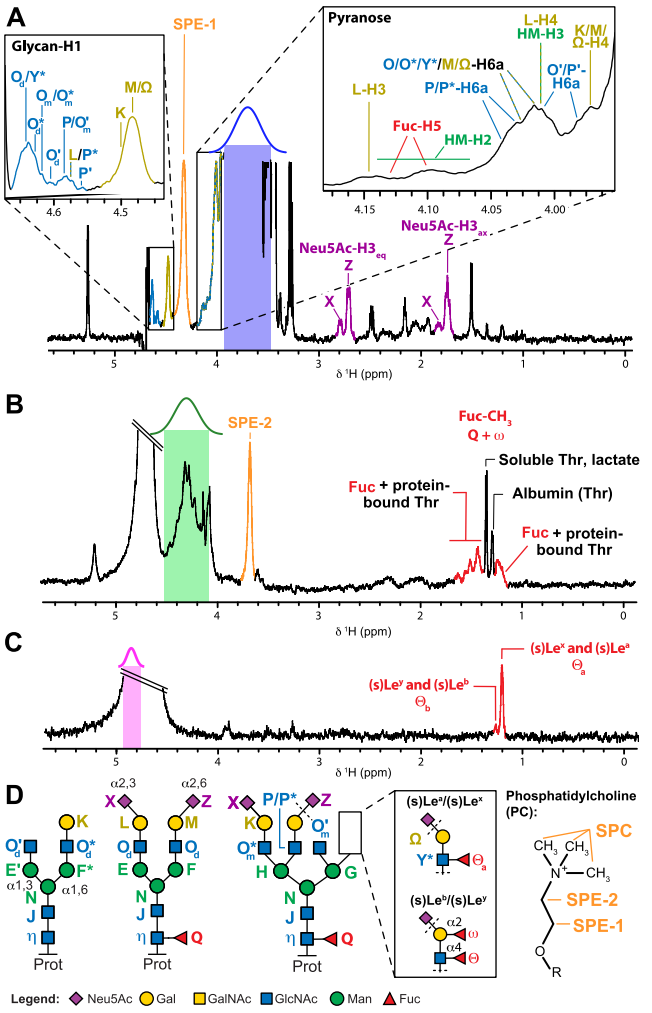

Figure 3. Assignment of *N*-glycan signals in selTOCSY spectra from a plasma sample selectively excited at (A) 3.7 ppm, (B) 4.3 ppm, and (C) 4.85 ppm. Blue, green, and pink areas represent the effective excitation field achieved in the corresponding experiments. (D) Cartoon representation of representative *N*-glycans and Lewis. The chemical structure of PC indicating the protons giving rise to SPC, SPE-1, and SPE-2. R indicates the rest of the molecule.

assess PC concentration (Figure S13).[42] Therefore, selTOCSY offers an attractive alternative for quantification of PC as a biomarker compared to the previously described approaches. Moreover, selTOCSY-4.3 also reveals protein threonine methyl groups (Thr-CH_3). (Figure 3B) Such markers display protein-specific patterns, providing an alternative avenue for glycoprotein differentiation.

We have also compared selTOCSY profiles from serum with those measured from plasma. As expected, glycoprofiles were virtually identical except for signals from fibrinogen, which were absent in plasma (Figure S14). To be suitable for fast screening, we optimized selTOCSY acquisition for fast relaxing *N*-glycan signals, as reported in Figures S15−S19 and Table S7 in the Supporting Information.

Enzyme Digestions of Serum Samples Confirm NMR Assignments. Assignments of *N*-glycan signals detected in selTOCSY spectra from serum samples are based on comparisons with our *N*-glycan standards. Chemical shifts of *N*-glycan signals arising from glycoproteins are insensitive to variations in pH and NaCl typically observed in serum and plasma (Figures S20 and S21). However, their chemical shifts may be altered owing to the protein environment. Consequently, we decided to confirm our assignments by employing selective glycoside hydrolases to sequentially digest the glycans of serum glycoproteins directly in serum samples. Enzyme digestions were monitored by NMR selTOCSYs after removal of released glycans by size exclusion chromatography.

In a first step, we studied the anomeric signals observed in selTOCSY-3.7 (Figure 4A, top spectrum). Overnight neuraminidase treatment of serum removed the signals corresponding to Neu5Ac-H3, therefore confirming this assignment (Figure 4A, middle spectrum). Subsequent treatment with β1,4-galactosidase S produced a spectrum devoid of the Gal-H1 signal (K) (Figure 4A, bottom spectrum). For more details, see Figure S22.

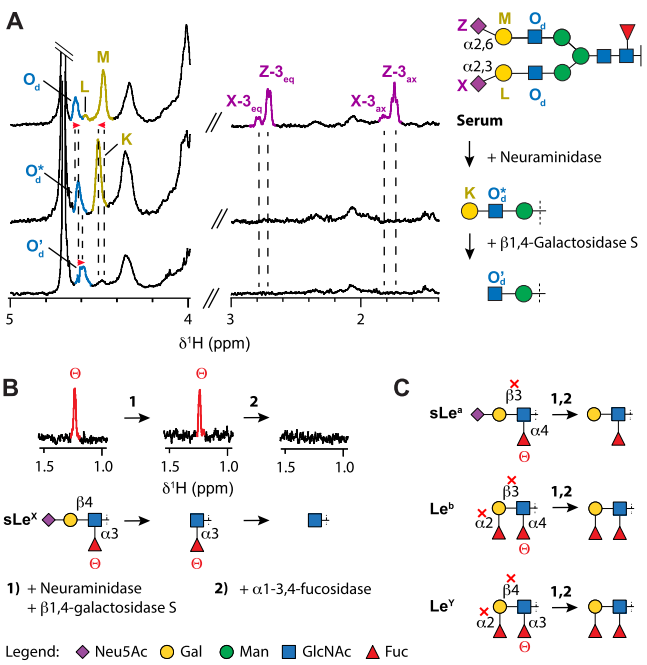

Figure 4. Identification of serum *N*-glycan signals in selTOCSY experiments using selective enzymatic digestions. (A) Identification of antennae anomeric signals in selTOCSY-3.7. The serum sample was treated with neuraminidase followed by β1,4-galactosidase S. (B) Treatment of a serum sample with a mixture of neuraminidase and β1,4-galactosidase S followed by α1-3,4-fucosidase removes the Fuc-CH_3 signal in selTOCSY-4.85, revealing the identity of the signal as (s)Le^x. (C) Fuc-Θ cannot be removed from (s)Le^a, Le^b, and Le^y using this enzymatic cocktail. Red crosses indicate noncleavable glycosidic bonds.

Considering the importance of (s)Le^x and (s)Le^a, we also examined the Fuc-CH_3 signal observed at 1.18 ppm in selTOCSY-4.85. Based on our reference glycans, we assigned this signal to sialylated and nonsialylated Le^x and Le^a antigens (Figures S7 and S8). To confirm the assignment in samples from the cancer patient cohort, we treated a serum sample from an HCC patient using a cocktail of enzymes. In a first step, Neu5Ac and Gal were removed by treatment with neuraminidase and β1,4-galactosidase S (Figure 4B). Treatment with neuraminidase removing terminal Neu5Ac is necessary because β1,4-galactosidase S only cleaves terminal Gal. Importantly, β1,3-linked Gal present in Le^a and fucosylated Gal present in Le^b and Le^y are not cleaved by this enzyme (Figure 4C).

https://doi.org/10.1021/acs.analchem.5c00285
Anal. Chem. 2025, 97, 9367−9377

Subsequent treatment with α1-3,4-fucosidase produced a spectrum devoid of Fuc-CH_3, confirming the identity of the signal as (s)Le^x. Fuc bound to GlcNAc in (s)Le^a, Le^b, and Le^y is not removed because α1-3,4-fucosidase only cleaves terminal Fuc. Importantly, the Fuc-CH_3 signal does not allow to distinguish between α1,4-linked Fuc present in (s)Le^a and those α1,3-linked Fuc in (s)Le^x. The two moieties can however be discriminated by targeting the anomeric proton, which yields a lower signal-to-noise signal. Further details are presented in Figure S23.

SelTOCSY-4.3 has also the potential to unveil signals from Fuc-CH_3 located in HBGA antigens (Figures S7 and S8). However, enzymatic treatment of serum samples with neuraminidase, β1,4-galactosidase S, and α1,2-fucosidase did not produce significant changes in selTOCSY spectra, suggesting low concentrations of HBGAs, as expected for serum samples (Figures S24 and S25).

We have also investigated optimal conditions for enzymatic digestions of core Fuc decorating native proteins. Unfortunately, in our hands, complete deglycosylation using PNGase F and PNGase A requires protein unfolding, rendering the samples unsuitable for NMR analysis. Nevertheless, specific signals from core Fuc moieties were identified from NMR spectra obtained from isolated serum glycoproteins. Further experiments can be found in Figures S26–S32.

Isolated Serum Glycoproteins Show Characteristic Glycoprofiles in SelTOCSY Spectra. For clinical diagnostic applications, discerning the contributions of individual acute-phase proteins to the overall glycoprotein glycan signal would be beneficial. To this end, we purified human serum glycoproteins from a healthy individual and acquired selTOCSY fingerprints. For this, it is critical to avoid protein denaturation. Therefore, we subjected serum glycoproteins isolated by UC to a series of mild isolation techniques, which included DEAE Affi-gel chromatography, size exclusion, ion exchange, and affinity chromatography. Using this methodology we have isolated nine acute-phase proteins: serotransferrin (TF), complement factor H (CFH), α2-macroglobulin (A2M), α1-antitrypsin (AAT), haptoglobin (HP), immunoglobulin A (IgA) and G (IgG), hemopexin (HPX), and human serum albumin (HSA).

Glycoprofiles arising from selTOCSY-3.7 provide information about antennae composition from prevalent *N*-glycans (Figure 5A). For all proteins, biantennary glycans were found to dominate glycoprofiles, in good agreement with previous work.[45] Distinct differences could also be observed as a function of the protein. For example, Neu5Ac(α2,3)Gal dominates in A2M, as can be seen from the Neu5Ac-H3 signals at ca. 2.8 ppm. This is also reflected in Gal-H1 and GlcNAc-H1 signals, which superimpose at ca. 4.55 ppm (* in Figure 5A). For IgA, a large content of nonsialylated, terminal Gal can be observed, as it is inferred from the shoulder in Gal-H1 signal (** in Figure 5A). IgG showed reduced signal intensity as a result of restricted glycan mobility in IgG, a consequence of intramolecular glycan–protein interactions.[46] Interestingly, AAT shows a unique signal from serine Hα at ca. 4.4 ppm with potential for protein identification (*** in Figure 5A). As expected, no glycan signals were observed for albumin owing to its lack of *N*-glycosylation sites.

SelTOCSY-4.3 produced unique profiles composed of signals from Fuc-CH_3 and also Thr-CH_3 groups (Figure 5B). Methyl signals are particularly useful for the analysis of blood samples, considering their high intensity and favorable

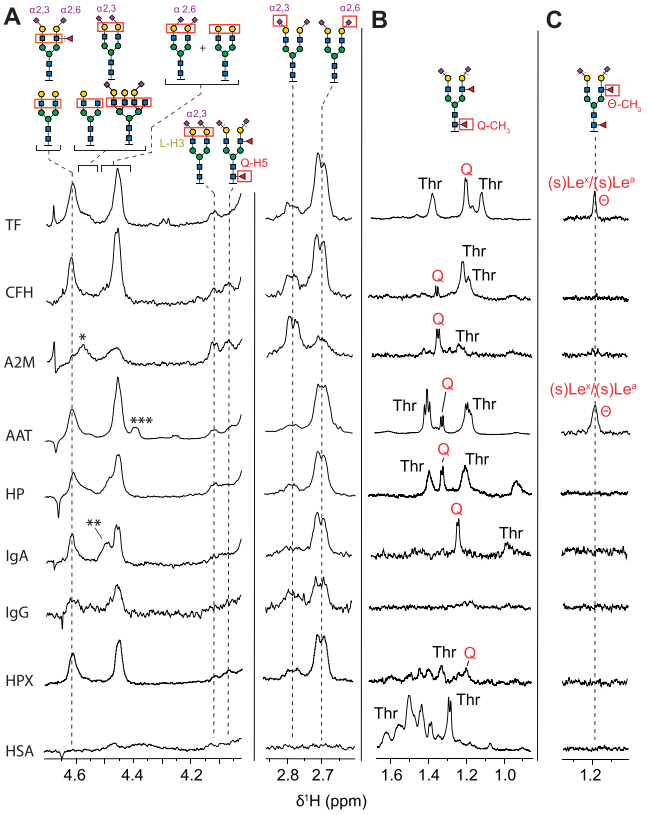

Figure 5. SelTOCSY NMR profiles of acute-phase glycoproteins isolated from human serum. Four selected spectral regions are shown, with excitation at three different frequencies (A) 3.70 ppm, (B) 4.30 ppm, and (C) 4.85 ppm. Orange boxes in glycan cartoons indicate the glycan part to which the NMR signal corresponds. Abbreviations of glycoproteins are indicated in the text. Thr denotes signals from threonine methyl groups.

relaxation properties. Fuc signals were assigned using a combination of 2D ^{1}H,^{1}H-TOCSY, and NOESY experiments, as illustrated in Figure S33. SelTOCSY-4.85 revealed the presence of (s)Le^x/(s)Le^a antigens in isolated TF and AAT samples (Figure 5C).

Glycosylation analysis by NMR bears additional challenges. The intensity of signals is not only a function of concentration but is also influenced by relaxation properties of glycans bound to proteins. Key factors that influence T_2 relaxation are the size of the protein (which correlates with the rotational correlation time τ_c) and the flexibility of glycan moieties on the surface of proteins. Such effects can be beneficial when discriminating between cohorts because they maximize differences in NMR glycan profiles. However, quantification of contributions of glycan signals from different proteins requires some sort of relaxation correction. To the best of our knowledge, no relaxation data are available for glycan residues decorating acute-phase proteins. Therefore, we have empirically calibrated glycan signals observed in NMR spectra of serum using UHPLC-MS as a reference method. We have also measured relaxation rates for the main glycan signals from the acute-phase proteins for calibration purposes (Tables S8 and S9).

NMR Glycoprofiles Contain Glycan-Specific Information. The ability to quantify spectral signals from specific *N*-glycans is central to NMR glycoprofiling. UHPLC-MS is widely regarded as standard for protein glycoprofiling.[47] Here, quantification is performed for the total released *N*-glycans,

https://doi.org/10.1021/acs.analchem.5c00285
Anal. Chem. 2025, 97, 9367−9377

independent of the glycosylation site. As absolute quantification is extremely challenging, current practice is to report the relative abundance of different glycoforms.

UHPLC results correlated well with NMR data. This is illustrated for GlcNAc-H1, Gal-H1, and Neu5Ac-H3eq NMR signals, which are all observed in selTOCSY-3.7, corresponding to glycan residues located in the antennae. These signatures exhibit the peculiar trait of small chemical shift differences as a function of the *N*-glycan structure. Spectra were analyzed by fitting series of Voigt lineshapes at different frequencies in selected spectral regions following a methodology previously established.[31] Positioning of the lineshapes was guided by knowledge gained from the NMR analysis of reference *N*-glycans (Figure 6A, reference *N*-glycans in Figures S2–S8).

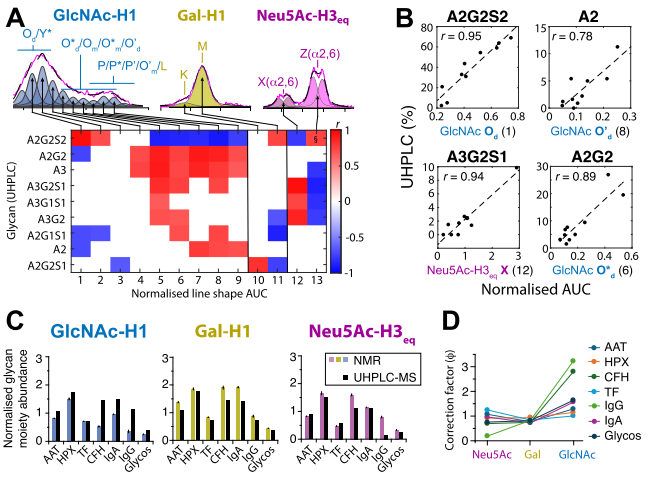

Figure 6. (A) Deconvolution of GlcNAc-H1 (blue), Gal-H1 (yellow), and Neu5Ac-H3eq (violet) NMR signals using lineshape fitting. AUCs for each lineshape were correlated with the relative *N*-glycan abundance observed by UHPLC-MS. Only significant correlations with a *p*-value < 0.05 are shown. § denotes a correlation with a *p*-value = 0.067. (B) Plots showing the correlation between the relative *N*-glycan abundance quantified by UHPLC vs normalized AUC of specific lineshapes from selTOCSY spectra. (C) Relative NMR quantification of *N*-glycan moieties located in the *N*-glycan antennae of isolated acute-phase proteins by NMR. Blue, yellow, and violet bars indicate the total content of GlcNAc, Gal, and Neu5Ac quantified by NMR according to eq 1 with Φ=1, while black bar corresponds to UHPLC. Errors indicate 95% margin of confidence. For glycos, n_{glyc} = 1. (D) Protein-specific correction factors Φ required to match UHPLC.

Areas under the curves (AUC) were normalized to the total spectral area (GlcNAc-H1 + Gal-H1 + Neu5Ac-H3eq) and subsequently correlated to relative glycan abundances obtained from UHPLC (Figure 6A,B). An excellent correlation of r > 0.95 was observed between the two analytical methods for the most abundant *N*-glycan A2G2S2. Moreover, very good correlations of r > 0.78 were obtained for less abundant *N*-glycans such as A3G2S1, A2G2, and A2. Importantly, NMR has the unique ability to discriminate between isobaric α2,3 and α2,6-Neu5Ac glycosidic bonds, which is only possible with linkage-specific derivatization for UHPLC-MS analysis.[48] Our analysis undoubtedly shows that α2,6-Neu5Ac is predominant in A2G2S2, while low-abundant triantennary A3G2S1 and A3G1S1 are rich in α2,3-Neu5Ac.

Glycoprotein *N*-glycan quantification from NMR spectra is affected by glycan-specific T_2 relaxation times. Therefore, we measured T_2 relaxation times for the signal envelopes GlcNAc-H1, Gal-H1, and Neu5Ac-H3eq for each isolated glycoprotein (Table S8). Protein-specific abundance ($A_{NMR,norm}$) values of antennae GlcNAc, Gal, and Neu5Ac were calculated from NMR spectra according to eq 1, which takes into account relaxation times of glycans and approximates relative abundances as observed in UHPLC analysis:

$$A_{\mathrm{NMR,norm}} = \frac{\frac{A_{\mathrm{signal}}}{e^{(-t/T_{2,\mathrm{signal}})}}}{\sum_{i=1}^{N}\frac{A_{\mathrm{signal},i}}{e^{(-t/T_{2,i})}}}\Phi n_{\mathrm{glyc}} \quad (1)$$

where A_{signal} represents the area of each signal envelope and t is the experimental time in selTOCSY during which spins are kept in the transverse plane prior to acquisition (65 ms). $T_{2,signal}$ represents the T_2 relaxation time determined for each specific signal envelope, Φ is a correction factor, and n_{glyc} is the total number of glycosites reported for the most abundant isoforms of each protein (Table S9). The index i runs from 1 to 3, corresponding to the number of signal envelopes analyzed for each glycoprotein (GlcNac-H1, Gal-H1, and NeuAc-H3). The denominator serves to obtain relative abundances to match the UHPLC data. Similarly, protein-specific abundances of antennae GlcNAc, Gal, and Neu5Ac were also calculated from UHPLC considering the sums of glycan residues arising from different glycans and glycosylation sites n_{glyc} from each protein. For details, see the Supporting Information.

Comparison of relative values between NMR and UHPLC shows very good agreement for AAT, HPX, and TF for the three glycan residues (Figure 6C). However, NMR values from CFH, IgA, and IgG deviate as a function of the residue. On average, NMR values increase as a function of the distance of the individual residue from the protein. For GlcNAc and Neu5Ac, abundances are being under- or overestimated, respectively, despite the relaxation correction. This is likely a consequence of mixed complexities of glycans with different T_2 values. This can be corrected by introducing a correction factor Φ required to match NMR and UHPLC outcomes (Figure 6D).

While there is a clear rationale on how to correlate UHPLC and NMR data, the key question is now whether there is an avenue to derive glycosylation biomarkers from mixtures in blood serum in spite of the challenges discussed, especially when individual relaxation rates cannot be determined.

Case Study—Hepatocellular Carcinoma (HCC) NMR Glycosylation Biomarkers. To determine whether NMR glycoprofiling is of potential clinical use, we have analyzed serum samples from a cohort of 33 HCC patients and 20 healthy controls. Three selTOCSY spectra were acquired per sample, with selective excitation frequencies as determined above (Figure 7A). A simple visual comparison between mean spectra obtained from HCC patients and healthy controls reveals clear differences in glycosylation patterns, particularly in core fucosylation, and in Fuc as part of (s)Le^x and (s)Le^a residues (Figure 7B and Figure S34).

SelTOCSY spectra were fitted with a series of Voigt lineshapes, as previously discussed. Statistically significant lineshapes and their corresponding associated glycosylation markers were identified based on Mann–Whitney U tests using the Benjamini, Krieger, and Yekutieli procedure for controlling the false discovery rate (Q = 0.05, see Figure S35 for more details). The largest differences between HCC and controls were observed in (i) Neu5Ac α2,6/α2,3 ratios, (ii) in

https://doi.org/10.1021/acs.analchem.5c00285
Anal. Chem. 2025, 97, 9367−9377

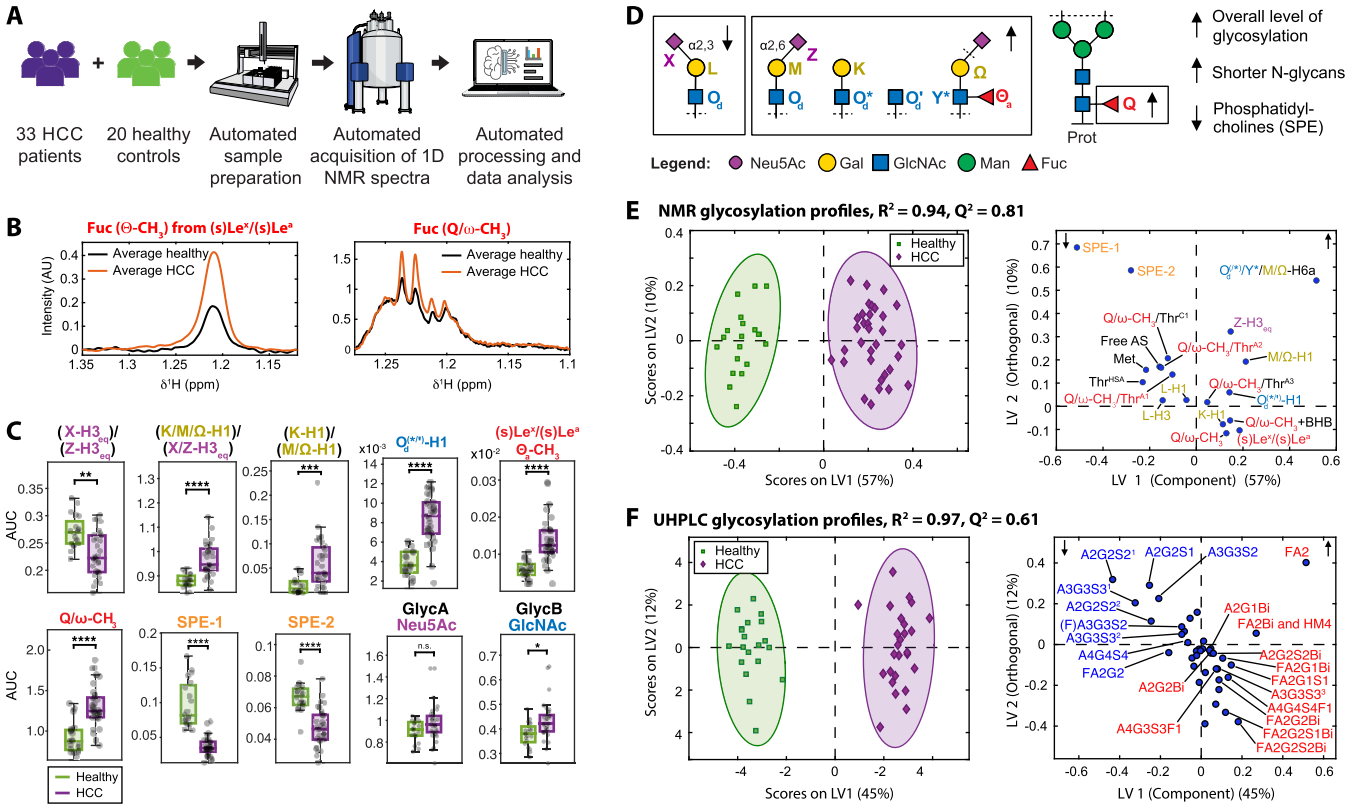

Figure 7. (A) Experimental design. Healthy controls are represented in green (n = 20) and hepatocellular carcinoma (HCC) patients in violet (n = 33). (B) Superimposition of average NMR spectra from healthy controls (black) and HCC (orange) from Fuc Lewis signal observed in selTOCSY-4.85 (left panel), and from core Fuc signals obtained from selTOCSY-4.3 (right panel). (C) Boxplots of relevant glycosylation features and ratios thereof. The asterisks *, **, ***, and **** correspond to q-values smaller than 0.05, 0.01, 0.001, and 0.0001, respectively. (D) Cartoon representation of significant changes in glycosylation profiles between HCC patients and healthy controls observed by NMR. Black arrows pointing upward and downward indicate an increase or decrease of corresponding glycan structures in serum from HCC patients as compared to healthy controls. (E, F) O-PLS-DA scores (left panels) and loadings (right panels) obtained when using (E) the 18 most significant selTOCSY markers and (F) serum glycosylation ratios obtained from UHPLC. The superscript in A2G2S2 and A3G3S3 in panel (F) denotes glycans with different combinations of α2,3 and α2,6-Neu5Ac bounds. Coefficients of determination of calibration data (R^2) and cross-validated data (Q^2) are indicated over the corresponding plots. Arrows in loading plots indicate values in HCC elevated as compared to healthy controls.

Neu5Ac/Gal ratios and Gal content, and (iii) in Neu5Ac/GlcNAc ratios. Similar differences are also seen for specific N-glycan branch content and in fucosylation patterns, as can be seen in Figure 7C for selected features, and in Figure S36.

As observed by selTOCSY analysis, the overall N-glycan content was elevated in HCC patients, with prevalence of biantennary over tri- or tetraantennary N-glycans. Glycoprofiles clearly indicate an increase in biantennary, short-branched N-glycans with antennae termed in Gal or GlcNAc.

Regarding sialic acid, a clear increase in α2,6 linked Neu5Ac can be observed in HCC samples. Moreover, significant changes in fucosylation patterns become apparent, with markedly elevated levels of core Fuc, (s)Le^x, and/or (s)Le^a (q < 0.0001, signals Fuc-Q-CH$_3$ and Fuc-ϑ-CH$_3$ in Figure 7B,C). The latter are of particular importance as established clinical biomarkers. Signals corresponding to protein-bound Thr produced a complex picture, likely reflecting changes in concentrations of hitherto unassigned acute-phase proteins. GlycA and GlycB did not allow for a differentiation between HCC and healthy controls. Finally, the concentration of PC (SPE-1 and SPE-2) was also found to be significantly lower in HCC patients. All these observations are summarized in Figure 7D.

The potential of NMR glycosylation profiles to discriminate between healthy controls and HCC samples is shown in Figure 7E. O-PLS-DA was carried out using the 19 most significant selTOCSY markers. Excellent cohort discrimination (R^2 = 0.94) was observed, with a cross-validated coefficient of determination (Q^2) of 0.81. Loading plots revealed that SPE and a complex array of glycosylation alterations are key to identifying HCC patients, indicating that cohort segregation is driven by a variety of N-glycan changes in circulating glycoproteins. Remarkably, O-PLS-DA based on glycosylation ratios obtained from UHPLC showed a nearly identical discrimination ratio of R^2 = 0.97, with a comparable Q^2 value of 0.61 (Figure 7E). Astonishingly, O-PLS-DA analysis of metabolite and lipoprotein signals led to a comparably poor discrimination with R^2 and Q^2 values of 0.66 and 0.55, respectively (Figure S37).

Altered glycosylation patterns observed by NMR are in excellent agreement with those observed by UHPLC, where sialylated and nonfucosylated N-glycans such as A2G2S2, A2G2S1, and A3G3S3 are clearly reduced in HCC patients (Figure S38). In contrast, fucosylated N-glycans with lower or no sialylation are predominant in HCC, with FA2 showing the most significant difference between the two cohorts (Figure 7F). Interestingly, HCC samples also show an increased prevalence of bisecting GlcNAc along several glycan types, in good agreement with previous reports.[49,50]

https://doi.org/10.1021/acs.analchem.5c00285
Anal. Chem. 2025, 97, 9367−9377

It is worth noting that changes in glycosylation patterns observed by NMR do not solely correspond to variations in protein concentrations. We have measured the concentrations of the most relevant acute-phase proteins involved in inflammatory and carcinogenic processes for the HCC and control samples. Comparison with glycosylation data showed that changes in protein concentrations capture only a fraction of the variance between cohorts, highlighting the potential of glycoprofiling to discriminate between healthy controls and HCC patients. This analysis is available in the Supporting Information, pg 53 and Figure S39. PCAs can be found in Figure S40, goodness of the models is described in Figures S41 and S42.

CONCLUSIONS

SelTOCSY emerges as a powerful NMR-based tool for glycoprotein analysis in blood, offering detailed glycan information with minimal sample preparation. Compared to traditional UHPLC-MS, it requires less effort yet reliably identifies key biomarkers, including critical sialic acid linkages (α-2,3 vs α-2,6-Neu5Ac) often missed during routine MS pretreatment. These linkages, along with high fucosylation levels, are essential indicators in diagnosing conditions such as HCC.

This approach significantly outperforms conventional GlycA/B NMR signals by providing a broader spectrum of glycosylation data, which enables near-complete differentiation between HCC and healthy samples. Despite potential signal relaxation challenges, selTOCSY consistently correlates well with UHPLC-MS findings and contributes valuable insights into prevalent glycan types. Ratios of glycosylation parameters, rather than absolute concentrations, enhance the reliability of these biomarkers across different platforms.

By integrating selTOCSY with metabolomics and lipoprotein profiling, rapid experimental workflows (under 30 min) become feasible. Future research will focus on characterizing glycan profiles of individual serum glycoproteins and examining larger patient cohorts to validate clinical utility. This includes exploring applications for early detection, as well as monitoring treatment response and relapse.

ASSOCIATED CONTENT

Supporting Information

The Supporting Information is available free of charge at https://pubs.acs.org/doi/10.1021/acs.analchem.5c00285.

Experimental protocols; NMR and selTOCSY spectra, enzyme kinetics, analysis of serum, assignment signals, irradiation, calibration, digestion, and statistical analysis (Figures S1−S42); other statistical data; and (Tables S1−S10) glycans used, list of 2D NMR experiments and enzymes, glycan signals, relaxation times, serum glycoproteins, and study population metrics (PDF)

UHPLC-MS data from isolated acute-phase glycoproteins, from HCC cohort and healthy controls (XLSX)

AUTHOR INFORMATION

Corresponding Authors

Ulrich L. Günther − *Institute of Chemistry and Metabolomics, University of Lübeck, Lübeck 23562, Germany;* orcid.org/0000-0001-9840-5943; Email: ulrich.guenther@uni-luebeck.de

Alvaro Mallagaray − *Institute of Chemistry and Metabolomics, University of Lübeck, Lübeck 23562, Germany;* orcid.org/0000-0001-5825-4407; Email: alvaro.mallagaraydebenito@uni-luebeck.com

Authors

Lorena Rudolph − *Institute of Chemistry and Metabolomics, University of Lübeck, Lübeck 23562, Germany; Institute of Clinical Chemistry and Laboratory Medicine, Carl von Ossietzky University, Oldenburg 26129, Germany;* orcid.org/0000-0002-0218-2747

Renia Krellmann − *Institute of Chemistry and Metabolomics, University of Lübeck, Lübeck 23562, Germany;* orcid.org/0009-0001-1860-9792

Darko Castven − *Medical Department I, University Medical Center Schleswig-Holstein, Lübeck 23538, Germany*

Lina Jegodzinski − *Medical Department I, University Medical Center Schleswig-Holstein, Lübeck 23538, Germany*

Helena Deriš − *Genos Glycoscience Research Laboratory, Zagreb 10000, Croatia*

Jerko Štambuk − *Genos Glycoscience Research Laboratory, Zagreb 10000, Croatia*

Jarne Mölbitz − *Institute of Chemistry and Metabolomics, University of Lübeck, Lübeck 23562, Germany*

Luna Dechent − *Institute of Chemistry and Metabolomics, University of Lübeck, Lübeck 23562, Germany*

Kai Sperling − *Institute of Chemistry and Metabolomics, University of Lübeck, Lübeck 23562, Germany*

Melissa Lindloge − *Institute of Chemistry and Metabolomics, University of Lübeck, Lübeck 23562, Germany;* orcid.org/0000-0001-9045-1902

Nele Friedrich − *Institute of Clinical Chemistry and Laboratory Medicine, Greifswald University Hospital, Greifswald 17475, Germany*

Franziska Schmelter − *Institute of Nutritional Medicine, University of Lübeck, Lübeck 23538, Germany*

Bandik Föh − *Institute of Nutritional Medicine, University of Lübeck, Lübeck 23538, Germany; Medical Department I, University Hospital Schleswig-Holstein, 23538 Lübeck, Germany*

Irena Trbojević-Akmačić − *Genos Glycoscience Research Laboratory, Zagreb 10000, Croatia;* orcid.org/0000-0003-0106-0155

Christian Sina − *Institute of Nutritional Medicine, University of Lübeck, Lübeck 23538, Germany; Medical Department I, University Hospital Schleswig-Holstein, 23538 Lübeck, Germany; Fraunhofer Research Institution for Individualized and Cell-Based Medical Engineering, Lübeck 23562, Germany*

Matthias Nauck − *Institute of Clinical Chemistry and Laboratory Medicine, Greifswald University Hospital, Greifswald 17475, Germany; German Center for Cardiogenic Vascular Research (DZHK), Partner Site Greifswald, University Medicine, Greifswald 17475, Germany*

Astrid Petersmann − *Institute of Clinical Chemistry and Laboratory Medicine, Carl von Ossietzky University, Oldenburg 26129, Germany; Institute of Clinical Chemistry and Laboratory Medicine, Greifswald University Hospital, Greifswald 17475, Germany*

Jens U. Marquardt − *Medical Department I, University Medical Center Schleswig-Holstein, Lübeck 23538, Germany*

Complete contact information is available at: https://pubs.acs.org/10.1021/acs.analchem.5c00285

https://doi.org/10.1021/acs.analchem.5c00285
Anal. Chem. 2025, 97, 9367−9377

Author Contributions

All authors have given approval to the final version of the manuscript.

Funding

We thank the VDI program of the BMBF (grant nos. 13GW0592E and REMOLCO) for support of this project and the EC for support under the ONCOSCREEN program (HORIZON-MISS-2021-CANCER-02, grant no. 101097036). We also thank the University of Lübeck, Germany, for the provision of facilities and resources that made this research possible.

Notes

The authors declare no competing financial interest.

■ ACKNOWLEDGMENTS

We would like to thank Prof. Thomas Peters (University of Lübeck, Germany) for helpful advice. We also thank Prof. Norbert Tautz and Dr. Olaf Isken (University of Lübeck, Germany) for granting us access to the facilities and equipment at the Institute of Virology.

■ REFERENCES

(1) Reily, C.; Stewart, T. J.; Renfrow, M. B.; Novak, J. *Nat. Rev. Nephrol* **2019**, *15*, 346−366.
(2) *The Role of Glycosylation in Health and Disease*; Lauc, G., Trbojević-Akmačić, I., Eds.; Advances in Experimental Medicine and Biology; Springer International Publishing: Cham, 2021; Vol. *1325*.
(3) De Haan, N.; Wuhrer, M.; Ruhaak, L. R. *Clinical Mass Spectrometry* **2020**, *18*, 1−12.
(4) Menni, C.; Gudelj, I.; Macdonald-Dunlop, E.; Mangino, M.; Zierer, J.; Bešić, E.; Joshi, P. K.; Trbojević-Akmačić, I.; Chowienczyk, P. J.; Spector, T. D.; Wilson, J. F.; Lauc, G.; Valdes, A. M. *Circ. Res.* **2018**, *122*, 1555−1564.
(5) Ohmichi, T.; Kasai, T.; Shinomoto, M.; Kitani-Morii, F.; Fujino, Y.; Menjo, K.; Mizuno, T. *PLoS One* **2023**, *18*, No. e0282153.
(6) Russell, A. C.; Šimurina, M.; Garcia, M. T.; Novokmet, M.; Wang, Y.; Rudan, I.; Campbell, H.; Lauc, G.; Thomas, M. G.; Wang, W. *Glycobiology* **2017**, *27*, 501−510.
(7) Xu, M.; Jin, H.; Wu, Z.; Han, Y.; Chen, J.; Mao, C.; Hao, P.; Zhang, X.; Liu, C.-F.; Yang, S. *ACS Chem. Neurosci.* **2022**, *13*, 1719−1726.
(8) Zhao, J.; Lang, M. *Cell Death Discovery* **2023**, *9*, 314.
(9) Tena, J.; Tang, X.; Zhou, Q.; Harvey, D.; Barajas-Mendoza, M.; Jin, L.; Maezawa, I.; Zivkovic, A. M.; Lebrilla, C. B. *Alz & Dem Diag Ass & Dis Mo* **2022**, *14*, No. e12309.
(10) Matsumoto, S.; Mashima, H. *Crohn's & Colitis 360* **2023**, *5*, No. otad028.
(11) Chen, R.; Chen, Q.; Zheng, J.; Zeng, Z.; Chen, M.; Li, L.; Zhang, S. *Cell Death Discovery* **2023**, *9*, 154.
(12) Ramachandran, P.; Xu, G.; Huang, H. H.; Rice, R.; Zhou, B.; Lindpaintner, K.; Serie, D. *J. Proteome Res.* **2022**, *21*, 1083−1094.
(13) He, K.; Baniasad, M.; Kwon, H.; Caval, T.; Xu, G.; Lebrilla, C.; Hommes, D. W.; Bertozzi, C. *J. Hematol Oncol* **2024**, *17*, 12.
(14) Wang, G.; Li, J.; Bojmar, L.; Chen, H.; Li, Z.; Tobias, G. C.; Hu, M.; Homan, E. A.; Lucotti, S.; Zhao, F.; Posada, V.; Oxley, P. R.; Cioffi, M.; Kim, H. S.; Wang, H.; Lauritzen, P.; Boudreau, N.; Shi, Z.; Burd, C. E.; Zippin, J. H.; Lo, J. C.; Pitt, G. S.; Hernandez, J.; Zambirinis, C. P.; Hollingsworth, M. A.; Grandgenett, P. M.; Jain, M.; Batra, S. K.; DiMaio, D. J.; Grem, J. L.; Klute, K. A.; Trippett, T. M.; Egeblad, M.; Paul, D.; Bromberg, J.; Kelsen, D.; Rajasekhar, V. K.; Healey, J. H.; Matei, I. R.; Jarnagin, W. R.; Schwartz, R. E.; Zhang, H.; Lyden, D. *Nature* **2023**, *618*, 374−382.
(15) Niu, L.; Geyer, P. E.; Wewer Albrechtsen, N. J.; Gluud, L. L.; Santos, A.; Doll, S.; Treit, P. V.; Holst, J. J.; Knop, F. K.; Vilsbøll, T.; Junker, A.; Sachs, S.; Stemmer, K.; Müller, T. D.; Tschöp, M. H.; Hofmann, S. M.; Mann, M. *Molecular Systems Biology* **2019**, *15*, No. e8793.
(16) Jiao, Y.; Xu, P.; Shi, H.; Chen, D.; Shi, H. *J. Cellular Molecular Medi* **2021**, *25*, 15−26.
(17) Duffy, M. J. *Ann. Clin Biochem* **1998**, *35* (Pt 3), 364−370.
(18) Ballehaninna, U. K.; Chamberlain, R. S. *J. Gastrointest. Oncol.* **2012**, *3*, 105.
(19) Mereiter, S.; Balmaña, M.; Campos, D.; Gomes, J.; Reis, C. A. *Cancer Cell* **2019**, *36*, 6−16.
(20) Visconti, A.; Rossi, N.; Deriš, H.; Lee, K. A.; Hanić, M.; Trbojević-Akmačić, I.; Thomas, A. M.; Bolte, L. A.; Björk, J. R.; Hooiveld-Noeken, J. S.; Board, R.; Harland, M.; Newton-Bishop, J.; Harries, M.; Sacco, J. J.; Lorigan, P.; Shaw, H. M.; de Vries, E. G. E.; Fehrmann, R. S. N.; Weersma, R. K.; Spector, T. D.; Nathan, P.; Hospers, G. A. P.; Sasieni, P.; Bataille, V.; Lauc, G.; Falchi, M. *BMC Cancer* **2023**, *23*, 166.
(21) Partyka, K.; Maupin, K. A.; Brand, R. E.; Haab, B. B. *Proteomics* **2012**, *12*, 2212−2220.
(22) Serdarevic, N. *Acta Inform Med.* **2018**, *26*, 235−239.
(23) Patabandige, M. W.; Pfeifer, L. D.; Nguyen, H. T.; Desaire, H. *Mass Spectrom. Rev.* **2022**, *41*, 901−921.
(24) Song, E.; Pyreddy, S.; Mechref, Y. *Rapid Commun. Mass Spectrom.* **2012**, *26*, 1941−1954.
(25) Schubert, M.; Walczak, M. J.; Aebi, M.; Wider, G. *Angew. Chem., Int. Ed.* **2015**, *54*, 7096−7100.
(26) Lenza, M. P.; Oyenarte, I.; Diercks, T.; Quintana, J. I.; Gimeno, A.; Coelho, H.; Diniz, A.; Peccati, F.; Delgado, S.; Bosch, A.; Valle, M.; Millet, O.; Abrescia, N. G. A.; Palazón, A.; Marcelo, F.; Jiménez-Osés, G.; Jiménez-Barbero, J.; Ardá, A.; Ereño-Orbea, J. *Angew. Chem. Int. Ed* **2020**, *59*, 23763−23771.
(27) Ala-Korpela, M.; Soininen, P.; Savolainen, M. J. *Circulation* **2009**, *120*, 931.
(28) Ala-Korpela, M.; Hiltunen, Y.; Jokisaari, J.; Eskelinen, S.; Kiviniitty, K.; Savolainen, M. J.; Kesäniemi, Y. A. *NMR Biomed.* **1993**, *6*, 225−233.
(29) Otvos, J. D.; Shalaurova, I.; Wolak-Dinsmore, J.; Connelly, M. A.; Mackey, R. H.; Stein, J. H.; Tracy, R. P. *Clinical Chemistry* **2015**, *61*, 714−723.
(30) Muhlestein, J. B.; May, H.; Winegar, D.; Rollo, J.; Connelly, M.; Otvos, J.; Anderson, J. *Journal of the American College of Cardiology* **2014**, *63*, A1389.
(31) Mallagaray, A.; Rudolph, L.; Lindloge, M.; Mölbitz, J.; Thomsen, H.; Schmelter, F.; Alhabash, M. W.; Abdullah, M. R.; Saraei, R.; Ehlers, M.; Graf, T.; Sina, C.; Petersmann, A.; Nauck, M.; Günther, U. L. *Angew. Chem., Int. Ed.* **2023**, *62*, No. e202306154.
(32) Lorenzo, C.; Festa, A.; Hanley, A. J.; Rewers, M. J.; Escalante, A.; Haffner, S. M. *Dia Care* **2017**, *40*, 375−382.
(33) Levine, J. A.; Han, J. M.; Wolska, A.; Wilson, S. R.; Patel, T. P.; Remaley, A. T.; Periwal, V.; Yanovski, J. A.; Demidowich, A. P. *Journal of Clinical Lipidology* **2020**, *14*, 667−674.
(34) Connelly, M. A.; Otvos, J. D.; Shalaurova, I.; Playford, M. P.; Mehta, N. N. *J. Transl. Med.* **2017**, *15*, 219−224.
(35) Fuertes-Martín, R.; Taverner, D.; Vallvé, J.-C.; Paredes, S.; Masana, L.; Correig Blanchar, X.; Amigó Grau, N. *J. Proteome Res.* **2018**, *17*, 3730−3739.
(36) Lodge, S.; Nitschke, P.; Kimhofer, T.; Wist, J.; Bong, S.-H.; Loo, R. L.; Masuda, R.; Begum, S.; Richards, T.; Lindon, J. C.; Bermel, W.; Reinsperger, T.; Schaefer, H.; Spraul, M.; Holmes, E.; Nicholson, J. K. *Anal. Chem.* **2021**, *93*, 3976−3986.
(37) Dona, A. C.; Jiménez, B.; Schäfer, H.; Humpfer, E.; Spraul, M.; Lewis, M. R.; Pearce, J. T. M.; Holmes, E.; Lindon, J. C.; Nicholson, J. K. *Anal. Chem.* **2014**, *86*, 9887−9894.
(38) Masuda, R.; Lodge, S.; Whiley, L.; Gray, N.; Lawler, N.; Nitschke, P.; Bong, S.-H.; Kimhofer, T.; Loo, R. L.; Boughton, B.; Zeng, A. X.; Hall, D.; Schaefer, H.; Spraul, M.; Dwivedi, G.; Yeap, B. B.; Diercks, T.; Bernardo-Seisdedos, G.; Mato, J. M.; Lindon, J. C.; Holmes, E.; Millet, O.; Wist, J.; Nicholson, J. K. *Anal. Chem.* **2022**, *94*, 4426−4436.

https://doi.org/10.1021/acs.analchem.5c00285
Anal. Chem. 2025, 97, 9367−9377

(39) Schumaker, V. N.; Puppione, D. L. [6] Sequential Flotation Ultracentrifugation. In *Methods in Enzymology*; Elsevier, 1986; Vol. *128*, pp 155−170.
(40) Trbojević Akmačić, I.; Ugrina, I.; Štambuk, J.; Gudelj, I.; Vučković, F.; Lauc, G.; Pučić-Baković, M. *Biochemistry Moscow* **2015**, *80*, 934−942.
(41) Šimunović, J.; GašPeršič, J.; Černigoj, U.; Vidič, J.; Štrancar, A.; Novokmet, M.; Razdorov, G.; Pezer, M.; Lauc, G.; Trbojević-Akmačić, I. *Biotech & Bioengineering* **2023**, *120*, 491−502.
(42) Nitschke, P.; Lodge, S.; Kimhofer, T.; Masuda, R.; Bong, S.-H.; Hall, D.; Schäfer, H.; Spraul, M.; Pompe, N.; Diercks, T.; Bernardo-Seisdedos, G.; Mato, J. M.; Millet, O.; Susic, D.; Henry, A.; El-Omar, E. M.; Holmes, E.; Lindon, J. C.; Nicholson, J. K.; Wist, J. *Anal. Chem.* **2022**, *94*, 1333−1341.
(43) Vliegenthart, J. F. G.; Dorland, L.; van Halbeek, H. High-Resolution, 1H-Nuclear Magnetic Resonance Spectroscopy as a Tool in the Structural Analysis of Carbohydrates Related to Glycoproteins. In *Adv. Carbohydr. Chem. Biochem.*; Tipson, R. S., Horton, D., Eds.; Academic Press, 1983; Vol. *41*, pp 209−374.
(44) Unione, L.; Lenza, M. P.; Ardá, A.; Urquiza, P.; Laín, A.; Falcón-Pérez, J. M.; Jiménez-Barbero, J.; Millet, O. *ACS Cent. Sci.* **2019**, *5*, 1554−1561.
(45) Clerc, F.; Reiding, K. R.; Jansen, B. C.; Kammeijer, G. S. M.; Bondt, A.; Wuhrer, M. *Glycoconj J.* **2016**, *33*, 309−343.
(46) Barb, A. W.; Meng, L.; Gao, Z.; Johnson, R. W.; Moremen, K.; Prestegard, J. H. *Biochemistry* **2012**, *51*, 4618−4626.
(47) de Haan, N.; Pučić-Baković, M.; Novokmet, M.; Falck, D.; Lageveen-Kammeijer, G.; Razdorov, G.; Vučković, F.; Trbojević-Akmačić, I.; Gornik, O.; Hanić, M.; Wuhrer, M.; Lauc, G.; The Human Glycome Project. *Glycobiology* **2022**, *32*, 651−663.
(48) Nishikaze, T. *Proc. Jpn. Acad., Ser. B* **2019**, *95*, 523−537.
(49) Somers, N.; Butaye, E.; Grossar, L.; Pauwels, N.; Geerts, A.; Raevens, S.; Lefere, S.; Devisscher, L.; Meuris, L.; Callewaert, N.; Van Vlierberghe, H.; Verhelst, X. *Oncol Lett.* **2024**, *29*, 24.
(50) Goldman, R.; Ressom, H. W.; Varghese, R. S.; Goldman, L.; Bascug, G.; Loffredo, C. A.; Abdel-Hamid, M.; Gouda, I.; Ezzat, S.; Kyselova, Z.; Mechref, Y.; Novotny, M. V. *Clin. Cancer Res.* **2009**, *15*, 1808−1813.

NOTE ADDED AFTER ASAP PUBLICATION

Due to a production error, the version of this paper that was published ASAP April 25, 2025, contained an errant space in the name of author Melissa Lindloge. The corrected version was posted May 6, 2025.

https://doi.org/10.1021/acs.analchem.5c00285
Anal. Chem. 2025, 97, 9367−9377